Geochemistry Geophysics Geosystems G3

Article
Volume 14, Number 10
24 October 2013
doi: 10.1002/ggge.20276
ISSN: 1525-2027

Published by AGU and the Geochemical Society

The active portion of the Campi Flegrei caldera structure imaged by 3-D inversion of gravity data

Paolo Capuano
Dipartimento di Fisica "E. R. Caianiello," Università degli Studi di Salerno, Via Giovanni Paolo II 132, 84084 Fisciano, Salerno, Italy (pcapuano@unisa.it)

Istituto Nazionale di Geofisica e Vulcanologia—Osservatorio Vesuviano, Napoli, Italy

Guido Russo
Dipartimento di Fisica, Università degli Studi di Napoli Federico II, Napoli, Italy

Lucia Civetta
Dipartimento di Scienze della Terra, dell'Ambiente e delle Risorse, Università degli Studi di Napoli Federico II, Napoli, Italy

Istituto Nazionale di Geofisica e Vulcanologia—Osservatorio Vesuviano, Napoli, Italy

Giovanni Orsi
Istituto Nazionale di Geofisica e Vulcanologia—Osservatorio Vesuviano, Napoli, Italy

Massimo D'Antonio
Dipartimento di Scienze della Terra, dell'Ambiente e delle Risorse, Università degli Studi di Napoli Federico II, Napoli, Italy

Istituto Nazionale di Geofisica e Vulcanologia—Osservatorio Vesuviano, Napoli, Italy

Roberto Moretti
Dipartimento di Ingegneria Civile, Design, Edilizia e Ambiente, Seconda Università degli Studi di Napoli, Aversa, Italy

Istituto Nazionale di Geofisica e Vulcanologia—Osservatorio Vesuviano, Napoli, Italy

Department of Geology, St. Mary's University, Halifax, Nova Scotia, Canada

[1] We present an improved density model and a new structural map of the Neapolitan Yellow Tuff caldera, the active portion of the nested Campi Flegrei caldera. The model was built using a new 3-D inversion of the available high-precision gravity data, and a new digital terrain and marine model. The inversion procedure, based on a variable-depth lumped assembling of the subsurface gravity distribution via cell aggregation, gives better defined insights into the internal caldera architecture, that well agree with the available geological, geophysical, and geochemical data. The adopted 3-D gravity method is highly efficient for characterizing the shallow caldera structure (down to 3 km depth) and defining features related to regional or volcano tectonic lineaments and dynamics. In particular, the resulting density distribution highlights a pronounced density low in correspondence of the central portion of the caldera with a detail not available till now. The joint interpretation of the available data suggests a subsurface structural setting that supports a piecemeal collapse of the caldera, and allows the identification of its headwall. Positive gravity anomalies localize dense intrusions (presently covered by

late volcanic deposits) along the caldera marginal faults, and the main structural lineaments both bordering the resurgent block and cutting the caldera floor. These results allow us to both refine the current geological-structural framework and propose a new structural map that highlights the caldera boundary and its internal setting. This map is useful to interpret the phenomena occurring during unrest, and to improve both short-term and long-term volcanic hazards assessment.

Components: 10,637 words, 6 figures.

Keywords: Campi Flegrei caldera; 3-D gravity inversion; Caldera collapse and resurgence.

Index Terms: 8440 Calderas: Volcanology; 1219 Gravity anomalies and Earth structure: Geodesy and Gravity; 0920 Gravity methods: Exploration Geophysics; 7205 Continental crust: Seismology; 7240 Subduction zones: Seismology; 0545 Modeling: Computational Geophysics; 1952 Modeling: Informatics; 4255 Numerical modeling: Oceanography: General; 4316 Physical modeling: Natural Hazards.

Received 25 June 2013; **Accepted** 20 September 2013; **Published** 24 October 2013.

Capuano, P., G. Russo, L. Civetta, G. Orsi, M. D'Antonio, and R. Moretti (2013), The active portion of the Campi Flegrei caldera structure imaged by 3-D inversion of gravity data, *Geochem. Geophys. Geosyst.*, *14*, 4681–4697, doi:10.1002/ggge.20276.

1. Introduction

[2] Formation and evolution of calderas, including precollapse tumescence and postcollapse resurgence, are still not fully understood and matter of scientific debate [*Newhall and Dzurisin*, 1988; *Lipman*, 2000a; *Cole et al*., 2005]. According to geometry of their collapse, calderas have been categorized in five end-members (see the review by *Cole et al*. [2005]). In particular, piecemeal collapse calderas are characterized by numerous floor blocks and/or multiple collapse centers [*Branney and Kokelaar*, 1994; *Moore and Kokelaar*, 1998]. Precollapse tumescence and postcollapse resurgence are very common processes associated with magmatic overpressure [*Lipman*, 2000b]. Caldera resurgence is triggered by overpressure reestablishment in the magma chamber after collapse [*Smith and Bailey*, 1968]. Its dynamics varies from doming [*Smith and Bailey*, 1968] to disjointing in differentially uplifted blocks [*Orsi et al*., 1991; *Acocella et al*., 2004] of the magma chamber roof rocks, and likely depends upon their aspect ratio [*Acocella et al*., 2001]. Hydrothermal reservoirs may play an important role during such processes [*Martí et al*., 2008].

[3] Geological, morphostructural, and petrological investigations of a given volcano help imaging its subsurface structural setting [*Bailey et al*., 1976; *Heiken et al*., 1990; *Orsi et al*., 1996; *Druitt et al*., 1999]. The detail of such an imaging depends upon availability of exposures of the internal part of the volcano, related to erosion depth. Advances in understanding calderas structure and collapse dynamics have resulted from the study of deeply eroded calderas such as Central San Juan and La Garita [*Lipman*, 2000a] and English Lake District [*Branney and Kokelaar*, 1994]. Furthermore, studies of magmatic volatiles [e.g., *Anderson et al*., 1989] allow us to assess both physicochemical state of magmatic systems [e.g., *Spilliaert et al*., 2006; *Mangiacapra et al*., 2008; *Arienzo et al*., 2010; *Moretti et al*., 2013a, 2013b] and thermobarometric conditions of the major magma storage levels through time.

[4] To construct a 3-D image of the internal structure of poorly eroded volcanoes, geophysical investigations can be regarded as a critical tool. 3-D images significantly contribute to validate the results of analog and numerical modeling of unrest, interpret the results of dynamic geophysical investigations, and assess the hazards posed by unrest [e.g., *Yokoyama and Mena*, 1991; *Davy and Caldwell*, 1998; *Beauducel et al*., 2004; *Gottsmann et al*., 2006; *Gottsmann and Battaglia*, 2008]. In particular, the study of the gravity field provides valuable information on the structure of volcanic systems, including collapse calderas, and, if repeated through time, their evolution [e.g., *Rymer*, 1994; *Yokoyama*, 1989; *Fournier et al*., 2004]. At collapse calderas (e.g., Long Valley, Valles, Toba), gravity imaging, together with P-T conditions constrained by volcanic gas geochemistry [e.g., *Giggenbach*, 1980], have provided important insights into their internal architecture, including likely magma batches and hydrothermal

reservoirs [e.g., *Sanders et al*., 1995; *Masturyono et al*., 2001].

[5] The Campi Flegrei caldera (CFc), located in the Campanian Plain, Southern Italy (Figures 1a and 1b), is a nested, resurgent, and restless structure in the densely inhabited Neapolitan area [*Orsi et al*., 1996]. The volcanic hazards posed by this caldera [*Orsi et al*., 2004, 2009; *Costa et al*., 2009; *Selva et al*., 2012] and the related risk are extremely high, because of its explosive character and the ~1.5 million people living within the caldera (~350,000 in its active portion). Since years the caldera is showing signs of unrest with ground uplift, seismicity, and composition variation of fumarole fluids, that have induced the Italian Department of Civil Protection to increase the alert level from "base" to "attention" (for updated information, visit www.ov.ingv.it and www.protezionecivile.it). In such a situation and for a better understanding of the ongoing unrest, the definition of the caldera structural setting and 3-D distribution of mass, including fluids, is of critical importance. To do so, we have performed the first fully 3-D inversion of gravity data collected over the past 30 years. The obtained results have enabled us to image the shallow subsurface density distribution of the Neapolitan Yellow Tuff (NYT) caldera, the youngest, resurgent and still active collapse structure of CFc, at the highest resolution ever achieved. They are presented and discussed together with results of previous geological, petrological, and geochemical studies, in order to better constrain the structure and present architecture of the caldera.

2. Geological Outlines

[6] CFc is composed of a subaerial and a submerged portion (Figure 1c). The horseshoe-shaped continental portion surrounding Pozzuoli Bay, includes many tuff-rings and tuff-cones, and is bounded Southward by the fossil marine cliff of the La Starza terrace [*Cinque et al*., 1985]. The submerged portion is characterized by a deeper South-western sector that extends South-eastward into the rectangular shaped, morphological low of Monte Dolce-Ammontatura (MD-A), delimited by the Pentapalummo Bank and Nisida Island morphological heights. To the West, two other volcanic fields occur, i.e. Procida and Ischia islands, the latter characterised by a multiple collapsed structure similar to that of CFc (see the review by *Paoletti et al*. [2013]).

[7] The Campi Flegrei depression has been variably interpreted. *Rosi et al*. [1983] and *Barberi et al*. [1991] suggested formation after a single caldera collapse accompanying the Campanian Ignimbrite (CI) eruption. *Lirer et al*. [1987] and *Scandone et al*. [1991] also attributed the depression to a single caldera collapse, but recognized the NYT eruption as the caldera-forming event. *Orsi et al*. [1992, 1996] first interpreted the depression as a nested caldera resulting from two major collapses related to CI (~39 ka; 300 km^3 of magma) and NYT (~15 ka; at least 40 km^3 of magma) eruptions [*Orsi et al*., 2004, and references therein]. *Acocella* [2008] and *Fedele et al*. [2011] corroborated this hypothesis. *Acocella* [2008] also suggested that both nested depressions were active during CI and NYT eruptions, with different downthrows.

[8] Large magma chambers at Campi Flegrei, as well as at Ischia and Somma-Vesuvius, have likely grown in crustal sectors in which intersecting NW-SE normal and NE-SW transtensive fault systems have generated high permeability [*Moretti et al*., 2013b, and references therein]. The NYT caldera (NYTc), nested within the CI caldera, produced the collapse of a ~90 km^2 area [*Orsi et al*., 1996] and was then the site of intense volcanism and block resurgence.

[9] Post-NYT volcanism generated more than 70 eruptions, grouped in three epochs of activity aged between 14.9 and 10.9 ka, 9.6 and 9.2 ka, and 5.6 and 4.2 ka, respectively [*Di Vito et al*., 1999; *Orsi et al*., 2004; *Di Renzo et al*., 2011]. Literature radiocarbon dates have been calibrated using the OxCal-Online software (https://c14.arch.ox.ac.uk) and the IntCal09 curve [*Reimer et al*., 2009]. Vent location through time has been used as a good tracer of the structural setting of the caldera. Those of the I and II epochs were located along the marginal faults of the caldera, while those of the III epoch were along that portion of the faults bordering the resurgent block [*Orsi et al*., 2004; *Selva et al*., 2012]. The Phlegraean magmas range in composition from shoshonite to phonolite. In the past 15 kyr, the magmatic system has included at least two crustal storage zones at variable depths. Shoshonitic to trachytic magmas residing, differentiating and degassing in a deep reservoir (7–9 km), either reached the surface along portions of NE-SW regional faults bordering the NYTc [*Orsi et al*., 1996] or raised to shallower reservoirs (5–4 km), where mingling/mixing with resident magmas, driven by a large gas phase, occurred [e.g., *D'Antonio et al*., 2007; *Mangiacapra et al*., 2008; *Arienzo et al*., 2010; *Tonarini et al*., 2009; *Di Renzo et al*., 2011, *Melluso et al*., 2012].

[10] Resurgence has been suggested to have occurred through a simple-shearing mechanism

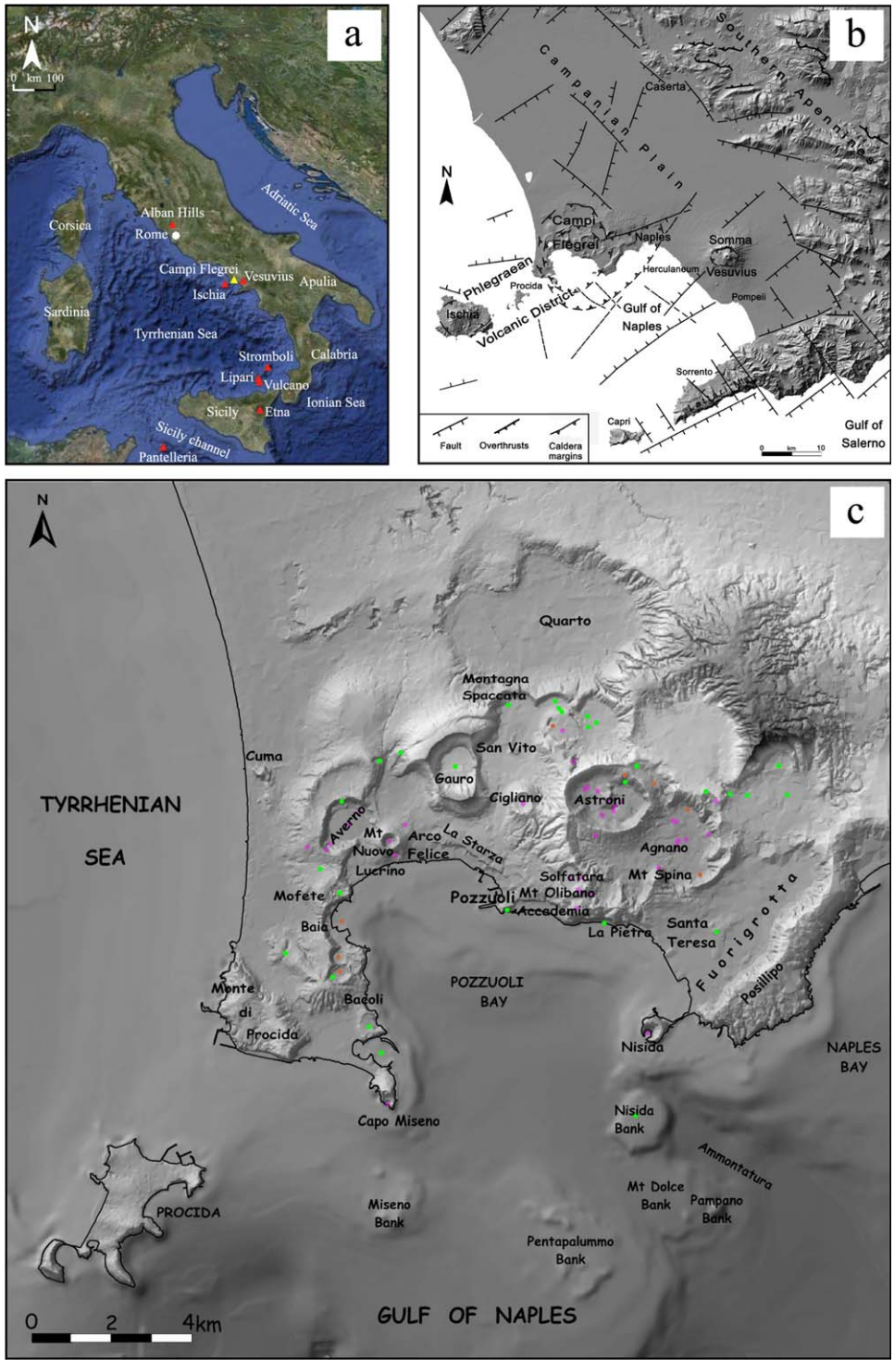

Figure 1. (a) Italy with its active volcanoes (as red triangles, except Campi Flegrei, in yellow), (b) structural sketch map of the Campanian Plain and surrounding Apennines, and (c) DTMM of the Campi Flegrei area. Solid dots are the volcanic vents of the first (green), second (brown), and third (magenta) epoch [*Orsi et al*., 2009].

[*Orsi et al*., 1991] that generated a maximum uplift of 90 m at La Starza marine terrace [*Cinque et al*., 1985] (Figure 1c) mainly through NE-SW and NW-SE faults [*Orsi et al*., 1996]. The eruption vents of both I and II epochs were located along the structural boundary of the NYTc. The last

epoch began after a significant change in the structural regime, that concentrated most eruption vents in the portion of the resurgent block under extension [*Di Vito et al*., 1999; *Orsi et al*., 1999a, 1999b, 2004; *Fedele et al*., 2011; *Selva et al*., 2012] (Figure 1c). The Agnano-Monte Spina eruption, the highest-magnitude event of this epoch, was accompanied by a volcano-tectonic collapse in the North-eastern part of the caldera [*de Vita et al*., 1999]. The last eruption occurred in AD 1538, after ~3 kyr of quiescence, and produced the Monte Nuovo tuff cone [*Guidoboni and Ciuccarelli*, 2011, and references therein]. This young eruption, widespread fumaroles and hot springs activity, and ongoing unrest, testify the persistent activity of the magmatic system. The unrest has produced at least two major (in 1969–1972 and 1982–1984) and many minor uplifts, interpreted as short-term transient episodes within the long-term resurgence process [*Orsi et al*., 1999a, 1999b]. The ground deformation generated by the 1982–1984 uplift can be reproduced by the upraise of about 60–70 $\times$ 10^6 m^3 of magma with a density of 2400 $kg \cdot m^{-3}$, compatible with that of volatile-rich trachybasaltic magma, rising from 7.5 to 5.5 km depth [*Trasatti et al*., 2011]. The deformation has also been interpreted as generated by injection and flow of geothermal fluids [*Bonafede*, 1991; *Battaglia et al*., 2006].

[11] Results of geophysical investigations and borehole drillings have contributed substantially to the definition of the caldera structure. *Cassano and La Torre* [1987] defined the main structural features through visual inspection of the gravity field and simple 2-D direct modeling of the results of the first gravity survey of the area. Integration of these results with deep drillings and magnetic survey data, permitted to relate a gravity low centered on Pozzuoli to a pyroclastic sequence with intercalated marine and continental sediments down to 2 km depth and overlying a thermometamorphic horizon [*AGIP*, 1987; *Barberi et al*., 1991]. The negative gravity anomaly was interpreted as resulting from a funnel-shaped caldera with the bottom at about 3 km depth [*Fedi et al*., 1991]. A boundary analysis allowed *Florio et al*. [1999] to interpret the sharpest gradients associated with the Pozzuoli gravity low to the structural margins of a collapse caldera. It also highlighted E-W and NW-SE structures, within and bordering the caldera, respectively. *Berrino et al*. [2008] constructed several 2.5D gravity sections across the CFc, using an interpretative model including three main bodies with variable density: caldera filling sediments, local limestone basement, and crystalline basement. Denser rocks between 2 and 3 km depth have been interpreted as water-bearing and/or gas-bearing thermometamorphic rocks overlying the basement [*Judenherc and Zollo*, 2004; *Zollo et al*., 2008]. Furthermore, seismic reflection profiles suggest the occurrence of the Mesozoic limestone basement top at not-less-than 6 km depth [*Judenherc and Zollo*, 2004; *Vanorio et al*., 2006], and of a 1-km-thick, low-velocity layer, at about 8 km depth, interpreted as a partially molten zone [*Zollo et al*., 2008]. Seismic attenuation tomography highlights a possible small batch of melt, at 4–5 km depth, just below the area most uplifted during the 1982–1984 bradyseismic event [*De Siena et al*., 2010]. Temperature profiles measured in geothermal wells bored within the caldera show maximum values of about 350°C at about 2.5 km depth [*AGIP*, 1987].

[12] CFc includes a large and vigorously active hydrothermal system [e.g., *Caliro et al*., 2007; *Chiodini et al*., 2012], which surface manifestations are concentrated in the areas mostly active since the III epoch (Figure 1c). The most vigorous manifestations are those of Solfatara and Pisciarelli, above an inferred isotherms rise zone [*Caliro et al*., 2007]. Borehole drillings have revealed overlying geothermal reservoirs between 1 and 3 km depth [*AGIP*, 1987], the deepest of which hosts high enthalpy (350–400°C), highly saline fluids. Nevertheless, the fluids released at Solfatara and Pisciarelli differ from the other Phlegraean discharges for their higher content of magmatic gases. Such a content testifies an underlying, degassing, magmatic body, releasing H_2O, CO_2, and acid gases that enter the hydrothermal system at ~2.5 km depth, at P-T conditions close to the critical point of pure water. Magmatic fluids mix with meteoric waters generating an ascending plume of hot gases from which steam condenses close to the surface, thus generating a water table emerging within the Agnano plain.

3. Gravity

[13] We have assembled in a single database the gravity data collected during several surveys at Campi Flegrei and their surroundings [*Maino and Tribalto*, 1971], the island of Procida [*Imbò et al*., 1964] and offshore in the Gulf of Naples [*Berrino et al*., 2008, and references therein]. Gravity data have been processed also using the first Digital Terrain Marine Model (DTMM) of the entire NYT

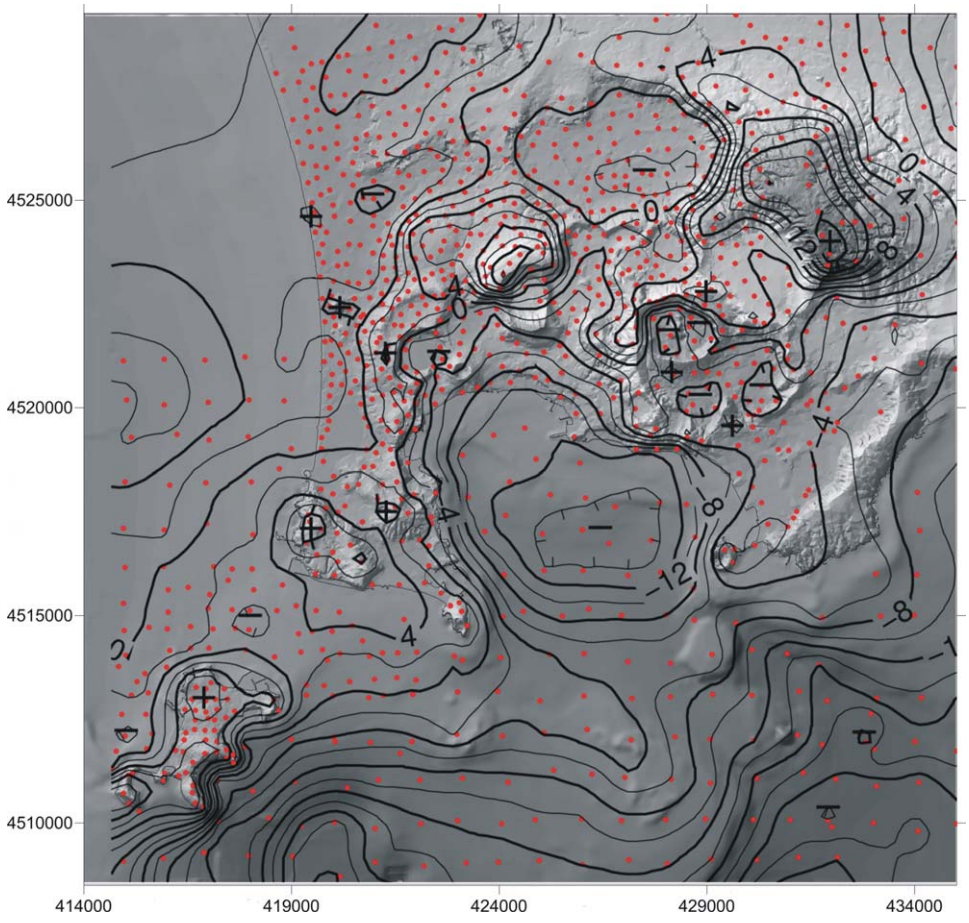

Figure 2. Faye anomaly map of the Campi Flegrei area, contoured at 2 mGal intervals. Red dots show the measurement locations.

caldera (20 × 20 m cell). The DTMM includes both subaerial and submerged portions of the structure and has been built using the largest available database of elevation data (topography, bathymetry, and gravity points elevations) (Figure 1c). The final product is a DTMM with an average grid resolution of 1 m and a maximum elevation error of 1 m.

[14] The reprocessed gravity anomaly map shows a minimum associated with the central portion of CFc, together with relative maxima along its margin and in the Camaldoli area (Figures 1 and 2). Rock densities have been evaluated by solving the resulting linear discrete inverse problem

$$A\mathbf{x} = \mathbf{b}$$

where A is the matrix of the gravity attraction generated by the blocks of our model, assumed having unit density, at data points, **x** is the vector of the unknown densities of the blocks, and **b** is the data vector, using the Tichonov regularization theory imposing on **x** the constraint of minimum norm [*Zhdanov*, 2002]. The strength of the method lays upon the used parameterization, based on triangular rather than rectangular prisms, and grouping procedures. On a planar scale, quasi-regular blocks of 0.85 × 0.85 km^2 have been constructed, while the topography has been reproduced by using a triangular mesh. The resulting model has a root mean square of 0.16 mGal. The misfit of the resulting solution (2×10^{-5} mGal in average) is very small over the entire area, but at a few locations where it can reach values as high as 1 mGal, indicating that some inconsistent data may still be in the data base (Figure 3).

[15] Low-density and high-density anomalies at the periphery of the surveyed area suffer from inaccuracies in the computational domain due to edge effects and are thus ignored in this paper. A resolution analysis shows that density is

well-resolved down to about 3 km depth. Details on data processing, gravity anomalies computation, and inversion procedure are reported in supporting information.[1]

4. 3-D Gravity Inversion Results

[17] The 3-D density distribution between sea level and 3000 m b.s.l. is highlighted through horizontal slices (Figure 4) cut at different depth, and variably oriented vertical cross sections (Figure 5). In the following, the density features characterizing the caldera at variable depth will be described.

[18] Above 200 m depth, the NYTc is characterized by positive and negative density anomalies (hereafter called anomalies) that, in its subaerial portion, mostly alternate in correspondence of lithologically different rock bodies (Figure 5). Between 200 and 600 m depth (Figures 4b and 5), the caldera is characterized mostly by negative anomalies. The Pozzuoli Bay and the MD-A morphological low are dominated by a density low about 6 km wide. Its Western portion includes a large wavelength, roughly N-S aligned and irregularly shaped density low. East of Baia a markedly N-S oriented positive anomaly occurs, extending to the coastline. Onshore, East of the Monte Nuovo cone, this positive anomaly continues into a N-S oriented negative anomaly. In the same sector N-S aligned, shorter wavelength relative density heights also occur. The North-North-eastern caldera sector is characterized by one positive and several short-wavelength negative anomalies. An E-W trending negative anomaly is located between Solfatara and Astroni.

[19] The 600–1000 m depth slice highlights density heights in correspondence of the area of recent volcanism, thus testifying the occurrence at shallow depth of high-density bodies remnant of dyke systems feeding such an activity. At this depth (Figures 4c and 5), the anomalies distribution identifies two different sectors within the caldera, subdivided by a NW-SE lineament roughly connecting Lucrino to Nisida. This lineament is also marked by alignments of fumaroles [*De Bonitatibus et al.*, 1970; *Orsi et al.*, 1996]. The South-western sector of the Pozzuoli Bay as well as the MD-A morphological low is largely dominated by negative anomalies, more accentuated than those at shallower depth. Those within the MD-A morphological low are clearly NW-SE elongated, while most of the anomalies at the South-western edge of the feature, align with those of the Pozzuoli Bay. Also in the North-eastern sector, the anomalies distribution does not change significantly, relatively to those at shallower depth. The E-W and N-S trending negative anomalies already highlighted at 200–600 m depth are more intense. A well-marked negative anomaly in the South-eastern portion of the Pozzuoli Bay is separated from two N-S aligned negative anomalies of similar intensity by a N-S lower intensity anomaly passing through Pozzuoli and cutting across the entire caldera (hereafter named Pozzuoli N-S negative anomaly).

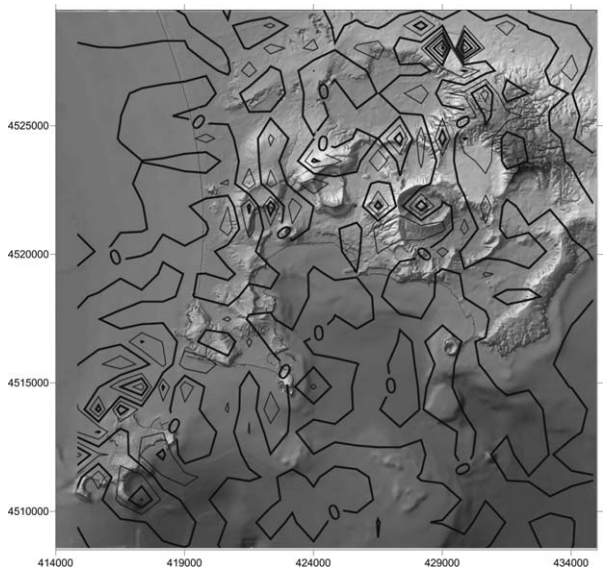

Figure 3. Gravity misfit of the computed anomaly with respect to the observed field. See text for details.

[20] Short-wavelength, positive anomalies occur mostly along the Eastern, Northern, and Western sectors of the caldera rim. They describe a pseudo-circular pattern that corresponds to alignments of the eruption vents of the I and II epochs, although they are outside the caldera collapsed area. Between Capo Miseno and Nisida these anomalies are attenuated. The negative anomalies of MD-A morphological low are bounded by two NW-SE alignments of positive anomalies. To the South-west is the pre-NYT Pentapalummo Bank anomaly, separated North-westward from the similarly trending Capo Miseno-Monte di Procida positive anomaly, by a small negative anomaly. To the North-east is the positive anomaly that extends from the South-western end of the Posillipo hill (Figure 1c), and corresponds to pre-NYT relict

[1]Additional supporting information may be found in the online version of this article.

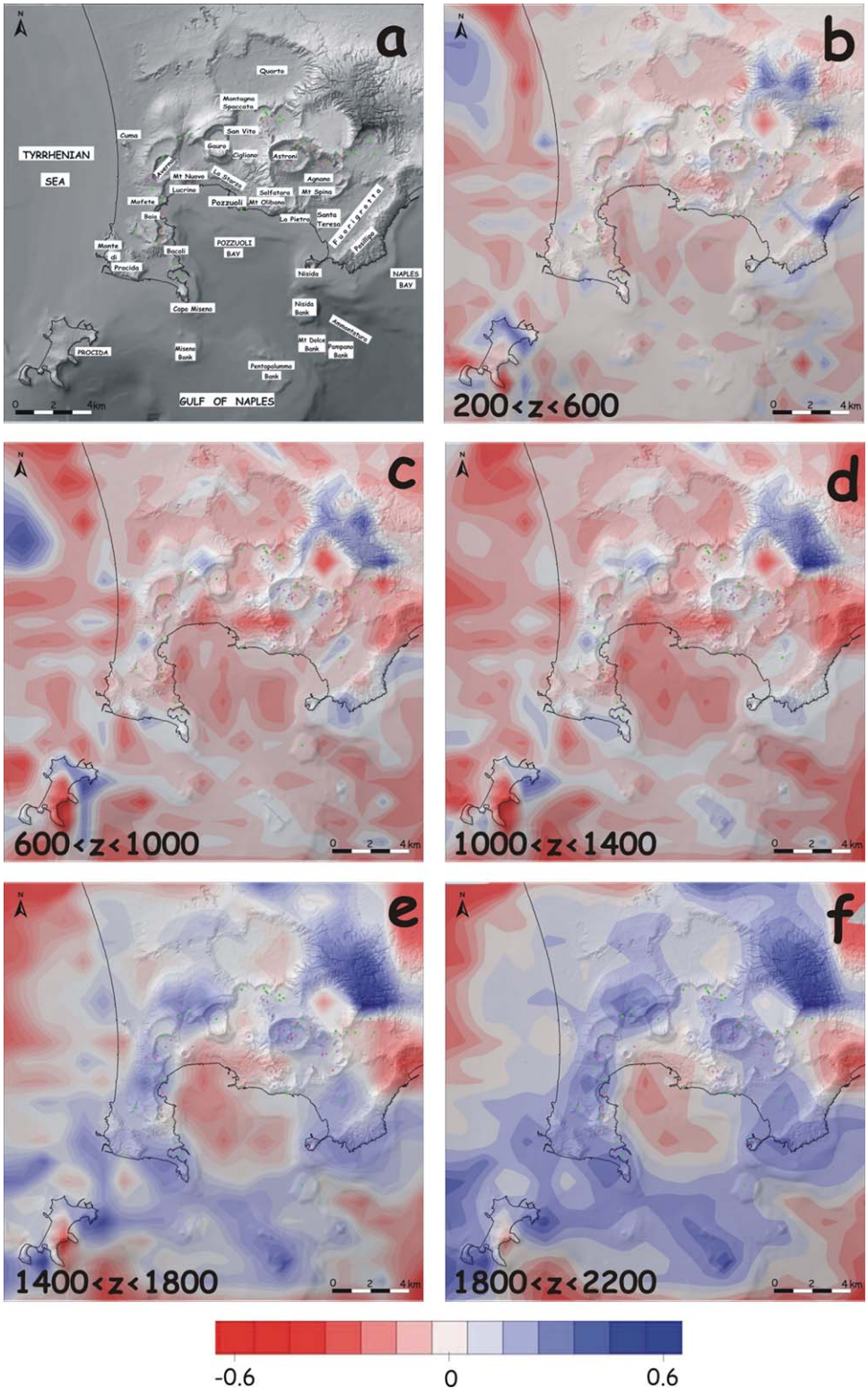

Figure 4. (a) DTMM of the Campi Flegrei area and (b–f) density horizontal slices at selected depth intervals. Solid dots are the volcanic vents of the first (green), second (brown), and third (magenta) epoch [*Orsi et al*., 2009]. Color scale represents density contrasts (g/cm^3).

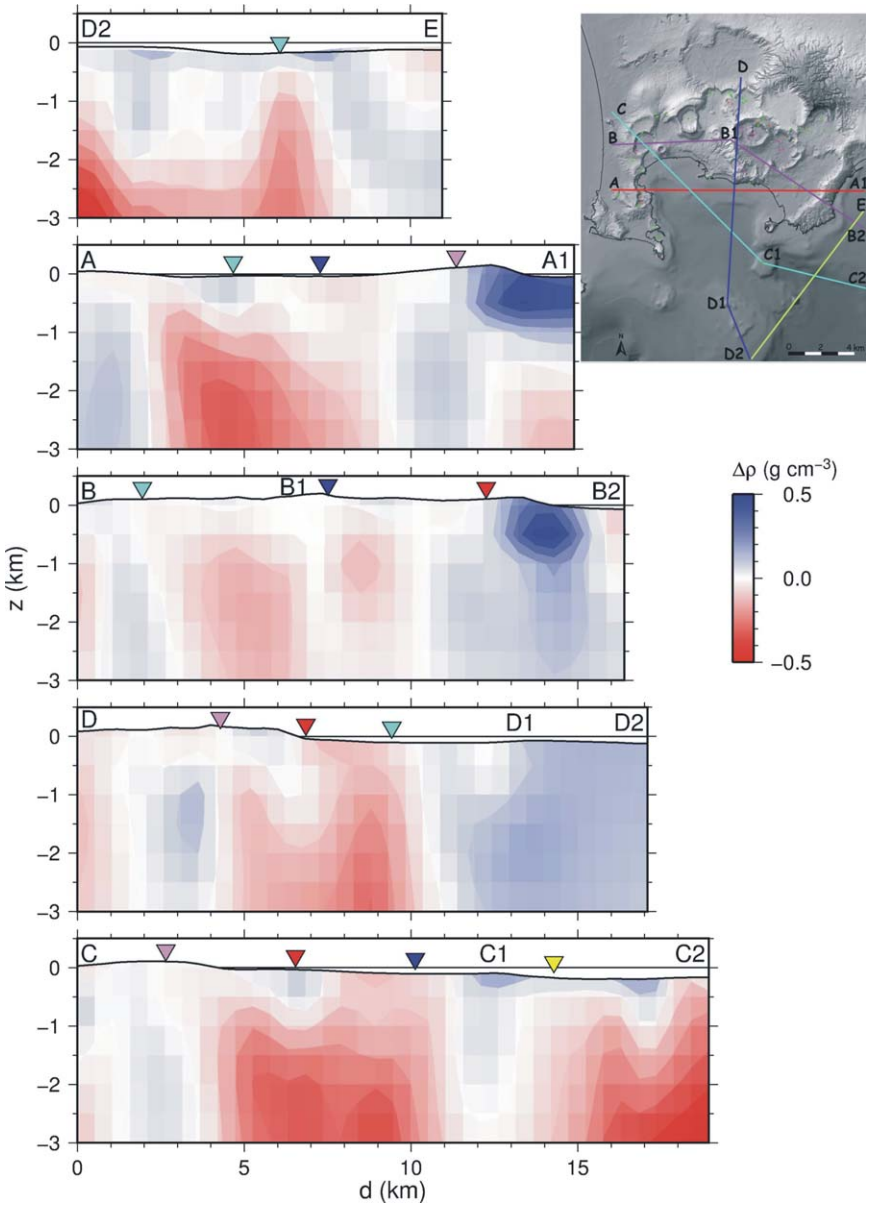

Figure 5. Selected vertical density cross sections. (top left) The trace of the plotted sections. Color scale represents density contrasts (g/cm^3).

centers. Two shallower positive anomalies are worth to be highlighted (Figures 4c and 5). One is located close to the Astroni volcano (III epoch) [*Tonarini et al*., 2009] and is adjacent to a similar-size positive anomaly to the South-east. The second is in the Fuorigrotta plain, close to the Santa Teresa volcanic center (I epoch), suggesting the occurrence of solidified poorly evolved magma at depth. The positive anomaly North of the Gauro volcano is much more pronounced than at shallower depth. Most of these features have been detected also by attenuation tomography and interpreted as solidified magma bodies [*De Siena et al*., 2010].

[21] Between 1000 and 1400 m depth (Figures 4d and 5), the negative anomalies of the South-western sector of the Pozzuoli Bay and the positive anomalies of the pseudo-circular feature, as well as the NW-SE Lucrino-Nisida alignment, are more accentuated. Also the anomalies of the Monte Dolce-Pampano feature and its shoulders are more accentuated. Furthermore, an almost continuous NE-SW trending short-wavelength

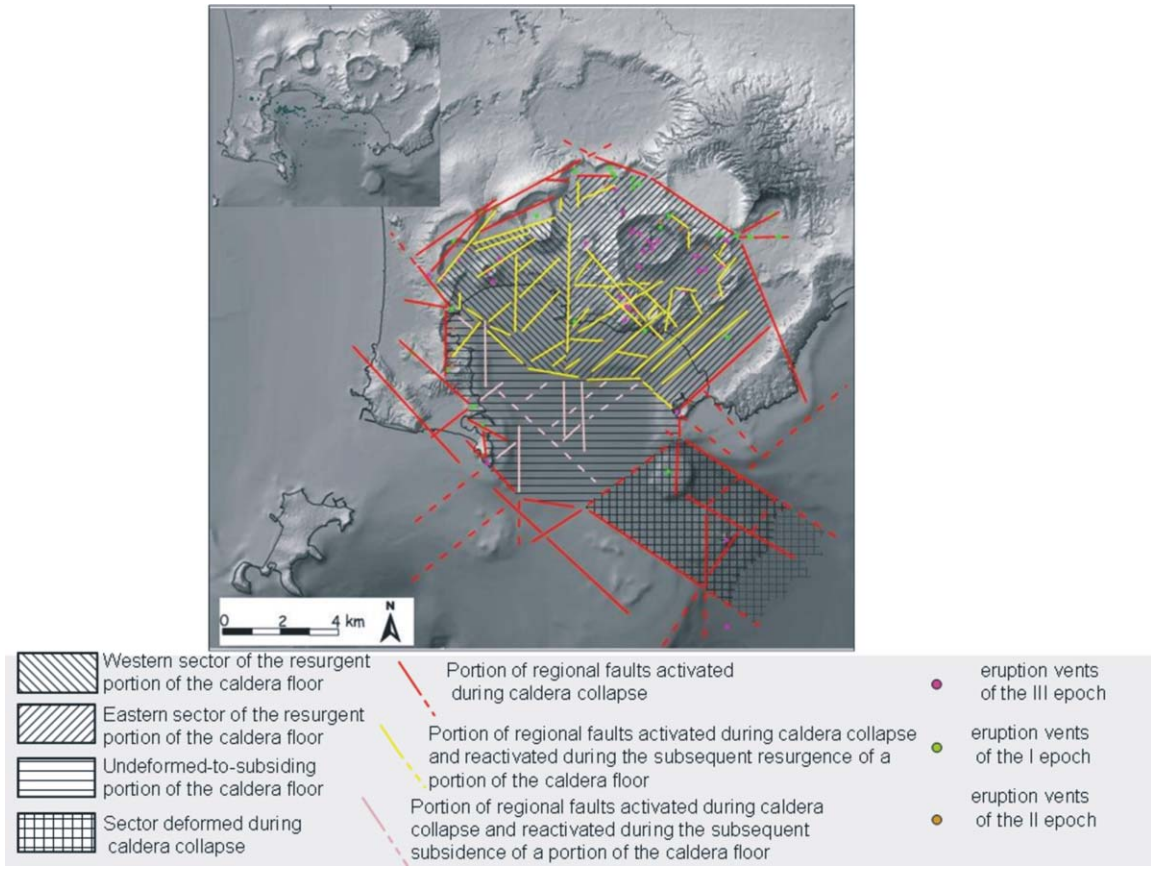

Figure 6. Structural sketch map of the Neapolitan Yellow Tuff caldera. The inset shows the distribution of the fumaroles; the offshore ones are from *De Bonitatibus et al*. [1970].

positive anomaly appears between this feature and the Pozzuoli Bay. The area from Posillipo to Astroni volcano is characterized by a relative positive anomaly, divided in two portions by a narrow, NE-SW elongated, relatively low-density anomaly that occurs in its central part and correlates with the South-eastern structural boundary of the resurgent block [*Orsi et al*., 1996, 1999a, 1999b]. The Northern portion of this density height has been the site of numerous vents of the III epoch, and of the volcano-tectonic Agnano-Monte Spina collapse [*de Vita et al*., 1999], while the Southern portion is characterized by the Santa Teresa volcano (I epoch). The positive anomaly South of Solfatara enlarges Southward. The structural boundary of the caldera is well marked by relative positive anomalies, testimonials of magma intrusions.

[22] Between 1400 and 1800 m depth (Figures 4e and 5) some of the gravity contrasts further sharpen, whereas other weaken, leading to a heterogeneous distribution of anomalies. In particular, the positive anomalies of the pseudo-circular feature further increase pointing to a continuous positive feature, while the negative anomalies in its central part become less intense and cover a smaller area. The MD-A feature is dominated by positive anomalies, with the negative ones only confined in the morphologically lowermost North-eastern portion. The negative anomaly West of Nisida is well separated from the other anomalies within the Pozzuoli Bay by the Pozzuoli N-S negative anomaly. The N-S negative anomaly East of Monte Nuovo extends Southward and its maximum is within the bay, between Mofete and Pozzuoli. The positive anomaly beneath the Fuorigrotta plain increases in intensity and size, and merges with the Astroni one. Conversely, both the N-S negative anomaly East of Monte Nuovo, and the E-W oriented one located between Solfatara and Astroni are less intense than at shallow depths. The positive anomaly South of Solfatara continues to enlarge and encompasses all the submerged area up to the E-W bending scarp and the Pozzuoli N-S negative anomaly.

[23] Below 1800 m depth (Figures 4f and 5), in the central portion of the Pozzuoli Bay, the two negative anomalies, although persisting, cover a still

smaller area, while in the MD-A low the positive anomalies become larger. The most striking difference with the areal distribution of the negative anomalies of the Pozzuoli Bay at shallower depth is that the minima, although still delimited by the Pozzuoli N-S negative anomaly and the E-W lineament that corresponds to the scarp South of the Pozzuoli-La Pietra coastline, are separated by a NE-SW lineament passing through the Monte Olibano-Solfatara area and continuing Southwestward up to Bacoli. The N-S lineament still persists North of the NE-SW one. The negative anomaly East of Mofete still persists, while the E-W oriented one between Solfatara and Astroni tends to disappear. The NW-SE lineament bordering the negative anomalies is well evident above 1600 m (Figures 4 and 5), whereas the NE-SW structure dominates below this depth, where it is the major divide between the two negative anomalies within the Pozzuoli Bay.

5. Discussion

[24] 3-D gravity imaging returns information useful to infer the distribution at depth of bodies with variable densities that can be validated by comparison with drilling logs. The 3-D anomalies distribution detected at CFc can be usefully compared to the stratigraphic sequences drilled at Mofete and San Vito [*AGIP*, 1987] (Figure 1c). In particular, the transition from negative to positive anomalies at $\sim$1400 and $>$600 m in the Mofete and San Vito areas, respectively, well matches the changes from tuffites and sedimentary material to lava flows and domes [*Rosi et al*., 1983]. Such a good match corroborates the effectiveness of the inversion method and its resolution, and permits a discussion on the results in terms of lithological characteristics of the rock bodies, current structural setting, and evolution of the caldera, as well as occurrence and distribution of the hydrothermal system.

[25] The caldera is located at the intersection of a dense network of NE-SW, NW-SE, N-S, and E-W trending gravity features (Figures 4–6), related to the regional tectonic lineaments of the Campanian Plain and the adjacent Apennine Chain (Figure 1b). The 3-D anomalies distribution sketches a pseudo-circular high-density feature, encompassing an inhomogeneous low-density crustal sector. The pseudo-circular feature shows a complexity in its South-eastern portion. Indeed, its continuity is interrupted as the MD-A morphological low is dominated by negative anomalies following a NW-SE alignment, well evident down to 1400 m depth. The root of this pseudo-circular anomalies alignment appears to extend down to 2000–3000 m at least, probably reaching an even greater depth (see deeper slices). The gravity lineaments are likely related to fault systems (Figure 6) highlighted also by geological, morphostructural, and geophysical investigations [*Cinque et al*., 1985; *Di Vito et al*., 1999; *Florio et al*., 1999; *Bruno*, 2004; *Judenherc and Zollo*, 2004; *Orsi et al*., 2009; *Sacchi et al*., 2009; *Acocella*, 2010; *Vilardo et al*., 2010]. The pseudo-circular feature corresponds to the caldera margin and begins to be evident at depth greater than 1000 m, while the low-density sector, characterizing the South-western portion of the Pozzuoli Bay, corresponds to the caldera fill (Figures 4–6). It is here hypothesized that the MD-A morphological low very likely formed during the deformation that generated the NYTc collapse.

[26] The high-density bodies responsible for the pseudo-circular feature are likely to be either remnants of the pre-NYT activity or shallow intrusions/feeding dykes mostly of the I and II epoch solidified within the marginal faults of the caldera (Figure 6) [*Orsi et al*., 1996, 2009, and references therein]. Lack of positive anomalies above 1600 m depth, in correspondence of the vents of some of these eruptions, suggests that after each explosive eruption the magma drained back into the partially emptied reservoir and the conduit was filled with low-density brecciated material. Outside the resurgent block, only the Nisida and Capo Miseno eruptions and likely the MD-A activity [*Sacchi et al*., 2009] have taken place during the III epoch along NW-SE structural lineaments. Nisida lies on the Lucrino-Nisida lineament, while Capo Miseno is located on the lineament that connects Monte di Procida to Pentapalummo Bank. MD-A activity has likely occurred at the intersection of elements of the NW-SE fault system of the MD-A morphostructural low, with N-S faults.

[27] The caldera fill is probably composed of a sequence of low-density trachytic and phonolitic pyroclastic deposits, intercalated with shallow sea sediments, as inferred from deep drilling data [*AGIP*, 1987; *Rosi et al*., 1983]. The rocks are affected by hydrothermal alteration [e.g., *Mormone et al*., 2011] that causes secondary void spaces and consequent bulk density lowering. The portion encompassed by the pseudo-circular high-density feature can be subdivided into a North-eastern and a South-western sector, according to the

distribution of anomalies. This subdivision is corroborated by the roughly NW-SE-trending morphostructural lineament connecting Lucrino to Nisida-Nisida Bank and delimiting North-eastward the MD-A morphostructural low (Figures 1c and 6), here called the Lucrino-Nisida lineament. We refer to the South-western deeper sector as the "undeformed-to-subsiding portion of the Pozzuoli Bay," and to the North-eastern shallower sector as the "resurgent portion of the caldera" (Figure 6). The Lucrino-Nisida lineament in the Pozzuoli Bay is an alignment of scarps that can be subdivided into three parts. The North-western and South-eastern parts are high-angle scarps, trending NW-SE and E-W, respectively. The central part is a more gentle slope scarp, intersected by NE-SW trending erosional features, likely testifying the occurrence of faults. South-east of Nisida it is again a NW-SE high-angle scarp. The Eastern and Western sides of the deeper sector of the Pozzuoli Bay are high-angle evolved flanks of volcanic edifices. The MD-A morphostructural low is composed of a series of faulted blocks which downthrow increases North-eastward. 3-D gravity imaging shows the persistence and even the enhancement of this feature at depth greater than 1800 m, thus involving the whole caldera down to its bottom. The "undeformed-to-subsiding portion of the Pozzuoli Bay" is characterized by a series of minima of different amplitude, down to about 1800 m depth, while the MD-A morphostructural low shows the same characteristics at shallower depth (1200 m; Figure 5). This pattern, likely resulting from blocks of different thickness and displaced at different depths by NW-SE, NE-SW, N-S, and E-W trending faults, suggests a piecemeal caldera collapse type, with the Pozzuoli Bay more downthrown than the MD-A morphostructural low.

[28] The resurgent portion of the caldera also shows a complex distribution of low-density and high-density bodies, reflecting the complex structural setting resulting from postcollapse resurgence and volcanism (Figure 6). The most striking features are relative density highs, and two N-S and one E-W oriented low-density anomalies. The areal correspondence of relative density heights and eruption vents of the III epoch also suggests the existence of a network of magmatic dykes that fed this activity. Good examples are the E-W positive anomaly East of Pozzuoli, in the Monte Olibano-Solfatara area (Figures 1c, 4, and 5), and the Agnano-Astroni and Monte Nuovo-Averno areas. The relative density height South of the Pozzuoli-La Pietra coastline is likely related to small-sized shallow intrusions related to magma upraise along the NE-SW structural lineament connecting Agnano to Monte Olibano-Accademia. The most prominent of the two N-S features is the complex sequence of short-wavelength, low-density anomalies that forms the Pozzuoli N-S negative anomaly extending from 200 to 1800 m depth (Figures 1c and 4–6). The less prominent occurs East of Monte Nuovo. The E-W negative anomaly is located between Solfatara and Astroni volcanoes, and extends from the Agnano Plain to the Pozzuoli N-S negative anomaly. All these gravity features correspond to faults that either are marked by morphostructural lineaments or fluid emissions at surface, or have been detected by geophysical and/or geochemical investigations (Figure 6).

[29] Summarizing, it is worth noting that above 1800 m depth, the Pozzuoli N-S negative anomaly dominates the anomalies distribution through the entire caldera, from the Quarto Plain to its Southern margin (Figures 4 and 5). Below 1800 m depth, there is no more gravity evidence of this N-S lineament in correspondence of the Western end of the E-W scarp South of the Pozzuoli-La Pietra coastline (Figures 1 and 4).

[30] Within the North-eastern overall resurgent portion of the caldera, we distinguish at least two main sectors with variable behavior, separated by the previously described Pozzuoli N-S negative anomaly. Although both are affected by NE-SW and NW-SE trending fault systems, the Eastern and Western sectors are also significantly affected by E-W and N-S trending structures, respectively. The Eastern sector has been the site of most eruptions of the III epoch, and the Agnano-Monte Spina volcano-tectonic collapse, occurred mostly along NW-SE and NE-SW trending faults. The Solfatara-Monte Olibano-Accademia volcanism is also related to these two systems. Along the NE-SW structural lineament, and particularly at its intersection with a NW-SE one, magma rose toward the surface leaving high-density crystallized bodies in the crust, and erupting the poorly differentiated melts of the Monte Olibano and Accademia lava domes (Figure 1c). Prolongation of the NE-SW faults encompassing these eruption vents passes through the erosional features with similar direction at the edge of the roughly NW-SE aligned scarps delimiting the resurgent portion of the caldera South-westward (Figures 1c and 6). The Western sector includes the vents of the two Averno eruptions (III epoch) and that of Monte Nuovo. These vents are concentrated in its Western corner at the

junction of the major fault systems (NW-SE, NE-SW, and N-S). There is good evidence that the NE-SW and NW-SE structures have been the most active systems during collapse, although the N-S fault system has also played an important role in the collapse of the Western portion of the caldera. All these systems have also concurred to the post-collapse deformation.

[31] The sharp decrease in density at about 1800 m in the Pozzuoli Bay and at about 1200 m depth in the MD-A morphostructural low, likely representing the transition between the low-density caldera fill, and the relatively denser caldera headwall, marks the bottom of the structure. Accounting for the uncertainties related to both gravity and seismic data inversion, this transition could correspond to the discontinuity revealed by seismic tomography at about 2.7 km depth within the Pozzuoli Bay [*Vassallo et al*., 2010].

[32] Correlation of the gravity results with geodetic, geochemical, and seismic data acquired during the recent uplifting episodes, helps understanding their genetic processes. The low-density caldera fill (ca. 2 km thick) is the region in which the sharpest residual gravity changes have been detected during the last major unrest episode occurred in 1982–1984 [*Berrino et al*., 1992; *Gottsmann et al*., 2006], suggesting a direct relationship between negative anomalies and detected subsurface mass changes. Therefore, unrest episodes may be partly rooted in the low-density region, as previously suggested [*Trasatti et al*., 2011]. This region corresponds to the one with low-Vp/Vs ratio in the center of the caldera, likely made up of rocks containing over-pressurized gas (CO_2) [*Vanorio et al*., 2005; *De Siena et al*., 2010]. Its location down to 3 km depth corroborates the gravimetric findings as well as the hypothesis that the low-density anomaly is also due to the presence of a wide, gas-rich, low-density system. Remarkably, the low-density and low-Vp/Vs region seems to have a counterpart in the positive strain volume recently identified by *D'Auria et al*. [2012] and relative to a deep domain from which geothermal fluids are injected upward. Injection seems to occur through structural lineaments that correspond to the E-W Solfatara-Agnano and the N-S Arco Felice low-density features well recognizable above 1800 m depth, particularly between 600 and 1400 m (Figures 4). These anomalies match fairly well the residual surface geothermal gradient [*Corrado et al*., 1998; *de Lorenzo et al*., 2001], and corroborate the hypothesis that density contrasts in the central part of the caldera are also related to the presence of hydrothermal bodies releasing hot fluids upward, in addition to the disjointing in blocks of the caldera floor during collapse and subsequent deformation. Upraise of pressurized fluids may have been controlled by preexisting structural lineaments, which are compatible with both gravity contrasts and gradients of diffuse degassing of deep and highly-conservative components, such as helium [e.g., *Lombardi et al*., 1984].

[33] The E-W trending low-density region, dividing Astroni from Solfatara volcanoes (Figures 1c, 4, and 5), is presently not affected by surface gas discharge, in contrast with the Solfatara-Pisciarelli area that discharges the largest amount of magmatic gases of the entire CFc system [*Caliro et al*., 2007; *Chiodini et al*., 2010, 2012; *Moretti et al*., 2013b]. The magmatic fraction of these fluids is related to a 4–5 km deep degassing magma body, in agreement with attenuation tomography [*De Siena et al*., 2010], joint gravity and ground deformation modeling [*Trasatti et al*., 2011], and petrologic-geochemical modeling [*Moretti et al*., 2013b]. The E-W trending low-density region can result from a hydrothermal system extending between 1 and 2 km depth, sealed at its top by secondary minerals precipitation, to explain the lack of gas discharge at surface. Presence of such a hydrothermal system is corroborated by the occurrence of LP seismic events between 1000 and 2000 m depth in the area [*Saccorotti et al*., 2007; *Cusano et al*., 2008]. Conversely, sealing has been likely less effective at Solfatara-Pisciarelli area due to the occurrence of both a thick Solfatara crater filling [*Bruno et al*., 2007] and an ENE-WSW active fault system connecting Solfatara to Pisciarelli (Figure 6).

[34] Close to surface (0–200 m depth) larger errors affect the gravity data inversion. However, positive anomalies found in correspondence of actively degassing areas (e.g., Solfatara; Figures 4 and 5) can also be due to widespread precipitation of alteration minerals and filling of pores by hydrothermal liquids, in line with what is already suggested at a smaller scale to explain positive high-resolution Bouguer anomalies associated with Solfatara fumarolic discharges [*Bruno et al*., 2007].

6. Conclusions

[35] The first full 3-D inversion carried out on gravity data from the Phlegraean area enables better

insights into the structure of the NYT caldera, the still active, resurgent, and restless portion of the entire CFc. It highlights general features of the caldera such as major structural discontinuities that have acted as faults during both collapse and resurgence, caldera headwall, dense intrusive bodies, volcanic deposits, and highly fractured regions dominated by rising fluids. Furthermore, they constrain the dynamics of caldera collapse and resurgence, as well as the genesis of unrest episodes.

[36] Regional fault systems have played an important role in the definition of caldera boundary and disjointing of the caldera floor during both collapse and ongoing resurgence. The caldera structural boundary and the postcollapse deformation pattern support piecemeal collapse and block resurgence mechanisms. The caldera collapse occurred through reactivation of portions of preexisting faults as already suggested by *Orsi et al*. [1996]. The gravity data, together with the highly detailed DTMM and a reevaluation of the current literature, allow us to suggest that the collapse also involved the rectangular-shaped MD-A morphostructural low. This feature collapsed along portions of NW-SE faults that affected the Pentapalummo Bank and the volcanoes partially exposed at the South-western end of the Posillipo Hill. Very likely the collapse generated a series of faulted blocks with increasing downthrows Northeastward. This feature was intersected Northwestward by a NE-SW fault system that downthrew the Northern side, presently forming the "undeformed-to-subsiding portion of the Pozzuoli Bay." The remaining part of the caldera collapsed through NE-SW, NW-SE, N-S, and E-W faults. The distribution of small and shallow high-density bodies is consistent with intrusions along faults marking the caldera periphery. The caldera headwall is located at about 1800 and 1200 m depth, for the "undeformed-to-subsiding portion of the Pozzuoli Bay" and the MD-A morphostructural low, respectively, where the negative anomalies of its central part become less intense and cover a smaller area. The main structural lineaments, which have ruled the evolution of the caldera, have been preferential pathways for migration of aqueous fluids, gases, and magmas.

[37] The results of our study have allowed us to refine the structural setting of the resurgent block proposed by *Orsi et al*. [1996, 1999a]. The Northeastern resurging portion of the caldera can be subdivided in two sectors, separated by the N-S Pozzuoli lineament. In addition to the NE-SW and NW-SE trending fault systems, the Eastern and Western sectors are also significantly affected by E-W and N-S trending structures, respectively. During the III epoch most eruptions have occurred in the Eastern sector. Only the two Averno eruptions and the Monte Nuovo event have taken place in the Western sector. Outside the resurgent block only the Nisida and Capo Miseno eruptions have taken place during the III epoch. The vents of these eruptions are aligned along the NW-SE features. Nisida lies on the Lucrino-Nisida lineament that divides the "undeformed-to-subsiding portion" from the "resurging portion" of the caldera, while Capo Miseno is located on the lineament that connects Monte di Procida to Pentapalummo Bank. Nisida and Capo Miseno are at the edges of the Pozzuoli Bay, that is of the submerged portion of the caldera.

[38] The E-W low-density feature between Solfatara and Astroni testifies the occurrence of a low-density zone extending to about 2000 m depth, likely resulting from intense fracturing, prone to localized seismicity due to fluid injections detected prior to and during uplifting episodes [*Cusano et al*., 2008; *D'Auria et al*., 2011; *Chiodini et al*., 2012]. These fluids likely ascend from the bottom of the hydrothermal system (>2000 m depth), close to the critical point of water. However, lack of gas discharge at surface of the zone between Solfatara and Astroni might be explained by a sealing effect due to secondary minerals precipitation. Similar considerations can be developed for the N-S elongated negative anomaly East of Monte Nuovo, where the hydrothermal activity does not find a direct output to surface. Conversely, the intense fluid discharge at Solfatara-Pisciarelli area can be explained by a less effective sealing due to both a thick filling in the Solfatara crater [*Bruno et al*., 2007] and an ENE-WSW active fault system connecting Solfatara to Pisciarelli.

[39] The hydrothermal system beneath Solfatara is assumed to be fed by continuous magmatic degassing, the intensity of which periodically increases during volcanic unrest episodes. Because density changes are related to hot fluids injected from depth in the hydrothermal system, we suggest that at CFc gravimetric and thermal maps should represent a proxy of heat and fluid flux, especially in the 200–1000 m depth range, and their variations related to unrest. Therefore, our results allow us to improve both long-term and short-term volcanic hazards assessments, in relation to the caldera volcanic and deformation history, present structural setting, and

ongoing resurgence. Regarding long-term volcanic hazards assessment, the results contribute to a better understanding of the ongoing dynamics and hence a better definition of the areas more prone to vent opening in case of renewal of volcanism in short-mid terms. In relation to short-term volcanic hazards assessment, our results give a more detailed geological and hydrothermal framework for interpreting precursors phenomena. In addition, they can also help improving types and location of monitoring networks.

Acknowledgments

[40] The research has been carried out with the financial support of projects PRIN-COFIN 2008 (LC), INGV-DPC 2012-13, V_1 (GO), and INGV-DPC UNREST (PC). J. Tyburczy, M. Battaglia, and an anonymous reviewer are acknowledged for useful comments that have permitted to improve an early version of the manuscript.

References

Acocella, V. (2008), Activating and reactivating pairs of nested collapses during caldera forming eruptions: Campi Flegrei (Italy), *Geophys. Res. Lett.*, *35*, L17304, doi:10.1029/2008GL035078.

Acocella, V. (2010), Evaluating fracture patterns within a resurgent caldera: Campi Flegrei, Italy, *Bull. Volcanol.*, *72*, 623–638.

Acocella, V., F. Cifelli, and R. Funiciello (2001), The control of overburden thickness on resurgent domes: Insights from analogue models, *J. Volcanol. Geotherm. Res.*, *111*, 137–153.

Acocella, V., R. Funiciello, E. Marotta, G. Orsi, and S. de Vita (2004), The role of extensional structures on experimental calderas and resurgence, *J. Volcanol. Geotherm. Res.*, *129*, 199–217.

AGIP (1987), *Modello geotermico del sistema flegreo, Sintesi, Servizi Centrali per l'Esplorazione*, SERG-MESG, San Donato Milanese, 23 pp.

Anderson, A. T., Jr., S. Newman, S. N. Williams, T. H. Druitt, C. Skirius, and E. Stolper (1989), H_2O, CO_2, Cl and gas in Plinian and ash flow Bishop rhyolite, *Geology*, *17*, 221–225.

Arienzo, I., R. Moretti, L. Civetta, G. Orsi, and P. Papale (2010), The feeding system of Agnano-Monte Spina eruption (Campi Flegrei caldera, Italy): Dragging the past into present activity and future scenarios, *Chem. Geol.*, *270*, 135–147, doi:10.1016/j.chemgeo.2009.11.012.

Bailey, R. A., G. B. Dalrymple, and M. A. Lanphere (1976), Volcanism, structure, and geochronology of Long Valley caldera, Mono County, California, *J. Geophys. Res.*, *81*, 725–744.

Barberi, F., E. Cassano, P. La Torre, and A. Sbrana (1991), Structural evolution of Campi Flegrei Caldera in light of volcanological and geophysical data, *J. Volcanol. Geotherm. Res.*, *48*(1–2), 33–49.

Battaglia, M., C. Troise, F. Obrizzo, F. Pingue, and G. De Natale (2006), Evidence for fluid migration as the source of deformation at Campi Flegrei caldera (Italy), *Geophys. Res. Lett.*, *33*, L01307, doi:10.1029/2005GL024904.

Beauducel, F., G. De Natale, F. Obrizzo, and F. Pingue (2004), 3-D modelling of Campi Flegrei ground deformations: Role of caldera boundary discontinuities, *Pure Appl. Geophys.*, *161*(7), 1329–1344, doi:10.1007/s00024-004-2507-4.

Berrino, G., H. Rymer, G. C. Brown, and G. Corrado (1992), Gravity-height correlations for unrest at calderas, *J. Volcanol. Geotherm. Res.*, *53*, 11–26.

Berrino, G., G. Corrado, and U. Riccardi (2008), Sea gravity data in the Gulf of Naples. A contribution to delineating the structural pattern of the Phlegrean Volcanic District, *J. Volcanol. Geotherm. Res.*, *175*, 241–252, doi:10.1016/j.jvolgeores.2008.03.007.

Bonafede, M. (1991), Hot fluid migration: An efficient source of ground deformation: Application to the 1982–1985 crisis at Campi Flegrei-Italy, *J. Volcanol. Geotherm. Res.*, *48*, 187–198.

Branney, M. J., and B. P. Kokelaar (1994), Volcanotectonic faulting, soft-state deformation, and rheomorphism of tuffs during development of a piecemeal caldera, English Lake District, *Geol. Soc. Am. Bull.*, *106*, 507–530.

Bruno, P. P. (2004), Structure and evolution of the Bay of Pozzuoli (Italy) using marine seismic reflection data: Implications for collapse of the Campi Flegrei caldera, *Bull. Volcanol.*, *66*, 342–355, doi:10.1007/s00445-003-0316-9.

Bruno, P. P. G., G. P. Ricciardi, Z. Petrillo, V. Di Fiore, A. Troiano, and G. Chiodini (2007), Geophysical and hydrogeological experiments from a shallow hydrothermal system at Solfatara Volcano, Campi Flegrei, Italy: Response to caldera unrest, *J. Geophys. Res.*, *112*, B06201, doi:10.1029/2006JB004383.

Caliro, S., G. Chiodini, R. Moretti, R. Avino, D. Granieri, M. Russo, and J. Fiebi (2007), The origin of the fumaroles of La Solfatara (Campi Flegrei, South Italy), *Geochim. Cosmochim. Acta*, *71*, 3040–3055.

Cassano, E., and P. La Torre (1987), Geophysics, in *Phlegrean Fields: Quaderni de "La Ricerca Scientifica" 114* (9), edited by M. Rosi and A. Sbrana, pp. 94–103, CNR, Rome.

Chiodini, G., S. Caliro, P. De Martino, R. Avino, and F. Gherardi (2012), Early signals of new volcanic unrest at Campi Flegrei caldera? Insights from geochemical data and physical simulations, *Geology*, *40*(10), 943–946.

Cinque, A., G. Rolandi, and V. Zamparelli (1985), L'estensione dei depositi marini olocenici nei Campi Flegrei in relazione alla vulcano-tettonica, *Boll. Soc. Geol. Ital.*, *104*(2), 327–348.

Cole, J. W., D. M. Milner, and K. D. Spinks (2005), Calderas and caldera structures: A review, *Earth Sci. Rev.*, *69*, 1–26.

Corrado, G., S. de Lorenzo, F. Mongelli, A. Tramacere, and G. Zito (1998), Surface heat flow density at the Phlegrean fields caldera (southern Italy), *Geothermics*, *27*, 469–484.

Costa, A., F. Dell'Erba, M. Di Vito, R. Isaia, G. Macedonio, G. Orsi, and T. Pfeiffer (2009), Tephra fallout hazard assessment at the Campi Flegrei caldera (Italy), *Bull. Volcanol.*, *71*, 259–273, doi:10.1007/s00445-008-0220-3.

Cusano, P., S. Petrosino, and G. Saccorotti (2008), Hydrothermal origin for sustained Long-Period (LP) activity at Campi Flegrei Volcanic Complex, Italy, *J. Volcanol. Geotherm. Res.*, *177*(4), 1035–1044.

D'Antonio, M., S. Tonarini, I. Arienzo, L. Civetta, and V. Di Renzo (2007), Components and processes in the magma genesis of the Phlegrean Volcanic District (Southern Italy), in *Cenozoic Volcanism in the Mediterranean Area: Geol. Soc. Am. Spec. Pap. 418*, edited by L. Beccaluva, G. Bianchini and M. Wilson, pp. 203–220, Geol. Soc. Am., Boulder, CO or Colorado, doi:10.1130/2007.2418(10).

D'Auria, L., F. Giudicepietro, I. Aquino, G. Borriello, C. Del Gaudio, D. Lo Bascio, M. Martini, G. Ricciardi, P.

Ricciolino, and C. Ricco (2011), Repeated fluid-transfer episodes as a mechanism for the recent dynamics of Campi Flegrei caldera (1989–2010), *J. Geophys. Res.*, *116*, B04313, doi:10.1029/2010JB007837.

D'Auria, L., F. Giudicepietro, M. Martini, and R. Lanari (2012), The 4D imaging of the source of ground deformation at Campi Flegrei caldera (southern Italy), *J. Geophys. Res.*, *117*, B08209, doi:10.1029/2012JB009181.

Davy, B. W., and T. G. Caldwell (1998), Gravity, magnetic and seismic surveys of the caldera complex, Lake Taupo, North Island, New Zealand, *J. Volcanol. Geotherm. Res.*, *81*, 69–89.

De Bonitatibus, A., G. Latmiral, L. Mirabile, A. Palumbo, E. Sarpi, and A. Scalera (1970), Rilievi sismici per riflessione: Strutturali, ecografici (fumarole) e batimetrici nel Golfo di Pozzuoli, *Boll. Soc. Nat. Napoli*, *79*, 97–l15.

de Lorenzo, S., A. Zollo, and F. Mongelli (2001), Source parameters and three-dimensional attenuation structure from the inversion of microearthquake pulse width data: Qp imaging and inferences on the thermal state of Campi Flegrei caldera (southern Italy), *J. Geophys. Res.*, *106*, 16,265–16,286.

De Siena, L., E. Del Pezzo, and F. Bianco (2010), Seismic attenuation imaging of Campi Flegrei: Evidence of gas reservoirs, hydrothermal basins, and feeding systems, *J. Geophys. Res.*, *115*, B09312, doi:10.1029/2009JB006938.

de Vita, S., et al. (1999), The Agnano-Monte Spina eruption in the densely populated, restless Campi Flegrei caldera (Italy), *J. Volcanol. Geotherm. Res.*, *91*(2–4), 269–301.

Di Renzo, V., L. Civetta, M. D'Antonio, S. Tonarini, M. A. Di Vito, and G. Orsi (2011), The magmatic feeding system of the Campi Flegrei caldera: Architecture and temporal evolution, *Chem. Geol.*, *281*, 227–241, doi:10.1016/j.chemgeo.2010.12.010.

Di Vito, M. A., R. Isaia, G. Orsi, J. Southon, S. de Vita, M. D'Antonio, L. Pappalardo, and M. Piochi (1999), Volcanism and deformation in the past 12 ka at the Campi Flegrei caldera (Italy), *J. Volcanol. Geotherm. Res.*, *91*(2–4), 221–246.

Druitt, T. H., L. Edwards, R. M. Mellors, D. M. Pyle, R. S. J. Sparks, M. Lanphere, M. Davies, and B. Barreiro (1999), Santorini Volcano, *Geol. Soc. London Mem.*, *19*, 165 pp.

Fedele, L., D. D. Insinga, A. T. Calvert, V. Morra, A. Perrotta, and C. Scarpati (2011), $^{40}Ar/^{39}Ar$ dating of tuff vents in the Campi Flegrei caldera (southern Italy): Toward a new chronostratigraphic reconstruction of the Holocene volcanic activity, *Bull. Volcanol.*, *73*, 1323–1336, doi:10.1007/s00445-011-0478-8.

Fedi, M., C. Nunziata, and A. Rapolla (1991), The Campania-Campi Flegrei area: A contribution to discern the best structural model from gravity interpretation, *J. Volcanol. Geotherm. Res.*, *48*, 51–59.

Florio, G., M. Fedi, F. Cella, and A. Rapolla (1999), The Campanian plain and Phlegrean fields: Structural setting from potential field data, *J. Volcanol. Geotherm. Res.*, *91*, 361–379.

Fournier, N., H. Rymer, G. Williams-Jones, and J. Brenes (2004), High-resolution gravity survey: Investigation of subsurface structures at Poás volcano, Costa Rica, *Geophys. Res. Lett.*, *31*, L15602, doi:10.1029/2004GL020563.

Giggenbach, W. F. (1980), Geothermal gas equilibria, *Geochim. Cosmochim. Acta*, *44*, 2021–2032.

Gottsmann, J., and M. Battaglia (2008), Chapter 12—Deciphering causes of unrest at explosive collapse calderas: Recent advances and future challenges of joint time-lapse gravimetric and ground deformation studies, in *Caldera Volcanism: Analysis, Modelling and Response: Developments in Volcanology 10*, edited by J. Gottsmann and J. Martí, pp. 417–446, Elsevier.

Gottsmann, J., H. Rymer, and G. Berrino (2006), Unrest at the Campi Flegrei caldera (Italy): A critical evaluation of source parameters from geodetic data inversion, *J. Volcanol. Geotherm. Res.*, *150*, 132–145.

Guidoboni, E., and C. Ciuccarelli (2011), The Campi Flegrei caldera: Historical revision and new data on seismic crises, bradyseisms, the Monte Nuovo eruption and ensuing earthquakes (twelfth century 1582 AD), *Bull. Volcanol.*, *73*(6), 655–677.

Heiken, G., F. Goff, J. N. Gardner, W. S. Baldridge, J. B. Hulen, and D. L. Nielson (1990), The Valles/Toledo caldera complex, Jemez volcanic field, New Mexico, *Annu. Rev. Earth Planet. Sci.*, *18*, 27–53.

Imbò, G., V. Bonasia, and P. Gasparini (1964), Rilievo gravimetrico dell'isola di Procida, *Ann. Oss. Vesuv.*, *6*, 117–138.

Judenherc, S., and A. Zollo (2004), The Bay of Naples (southern Italy): Constraints on the volcanic structures inferred from a dense seismic survey, *J. Geophys. Res.*, *109*, B10312, doi:10.1029/2003JB002876.

Lipman, P. W. (2000a), Calderas, in *Encyclopaedia of Volcanoes*, edited by H. Sigurdsson, pp. 643–662, Academic, San Francisco, Calif.

Lipman, P.W. (2000b), The central San Juan caldera cluster: Regional volcanic framework, *Geol. Soc. Am. Spec. Pap., 346*, pp. 9–71, Geol. Soc. Am., Boulder, Colo.

Lirer, L., G. Luongo, and R. Scandone (1987), On the volcanological evolution of Campi Flegrei, *Eos Trans. AGU*, *68*, 226–234.

Lombardi, S., M. Di Filippo, and L. Zantedeschi (1984), Helium in Phlegraean Fields soil gases: July 20th-26th–September 19th-25th, 1983, *Bull. Volcanol.*, *47*(2), 259–265.

Maino, A., and G. Tribalto (1971), Rilevamento gravimetrico di dettaglio dell'isola d'Ischia, Napoli, *Boll. Serv. Geol. Ital.*, *92*, 109–122.

Mangiacapra, A., R. Moretti, M. Rutherford, L. Civetta, G. Orsi, and P. Papale (2008), The deep magmatic system of the Campi Flegrei caldera (Italy), *Geophys. Res. Lett.*, *35*, L21304, doi:10.1029/2008GL035550.

Martí, J., A. Geyer, A. Folch, and J. Gottsmann (2008), Chapter 6—A review on collapse caldera modelling, in *Caldera Volcanism: Analysis, Modelling and Response: Developments in Volcanology 10*, edited by J. Gottsmann and J. Martí, pp. 233–283, Elsevier.

Masturyono, R. McCaffrey, D. A. Wark, S. W. Roecker, I. G. Fauzi, and Sukhyar (2001), Distribution of magma beneath Toba caldera complex, north Sumatra, Indonesia, constrained by three-dimensional P wave velocities, seismicity, and gravity, *Geochem. Geophys. Geosyst.*, *2*, 1014, doi:10.1029/2000GC000096.

Melluso, L., R. de' Gennaro, L. Fedele, L. Franciosi, and V. Morra (2012), Evidence of crystallization in residual, Cl-F-rich, agpaitic, trachyphonolitic magmas and primitive Mg-rich basalt-trachyphonolite interaction in the lava domes of the Phlegrean Fields (Italy), *Geol. Mag.*, *149*, 532–550, doi:10.1017/S0016756811000902.

Moore, I., and P. Kokelaar (1998), Tectonically controlled piecemeal caldera collapse: A case study of Glencoe volcano, Scotland, *Geol. Soc. Am. Bull.*, *110*, 1446–1466.

Moretti, R., I. Arienzo, L. Civetta, G. Orsi, and P. Papale (2013a), Multiple magma degassing sources at an explosive volcano, *Earth Planet. Sci. Lett.*, *367*, 95–104, doi:10.1016/j.epsl.2013.02.013.

Moretti, R., I. Arienzo, G. Orsi, L. Civetta, and M. D'Antonio (2013b), The deep plumbing system of the Ischia island (southern Italy): A physico-chemical and geodynamic window on the fluid-sustained and CO_2-dominated magmatic source of Campanian volcanoes, *J. Petrol.*, *54*(5), 951–984, doi:10.1093/petrology/egt002.

Mormone, A., A. Tramelli, M. A. Di Vito, M. Piochi, C. Troise, and G. De Natale (2011), Secondary hydrothermal minerals in buried rocks at the Campi Flegrei caldera, Italy: A possible tool to understand the rock-physics and to assess the state of the volcanic system, *Per. Mineral.*, *80*(3), 385–406.

Newhall, C. G., and D. Dzurisin (1988), Historical unrest at large calderas of the world, *U.S. Geol. Surv. Bull.*, *1855*(2), 1108 pp.

Orsi, G., L. Civetta, C. Del Gaudio, S. de Vita, M. A. Di Vito, R. Isaia, S. M. Petrazzuoli, G. Ricciardi, and C. Ricco (1999a), Short-term ground deformations and seismicity in the nested Campi Flegrei caldera (Italy): An example of active block-resurgence in a densely populated area, *J. Volcanol. Geotherm. Res.*, *91*(2–4), 415–451.

Orsi, G., M. D'Antonio, S. de Vita, and G. Gallo (1992), The Neapolitan Yellow Tuff, a large-magnitude trachytic phreatoplinian eruption: eruptive dynamics, magma withdrawal and caldera collapse, *J. Volcanol. Geotherm. Res.*, *53*, 275–287.

Orsi, G., S. de Vita, and M. Di Vito (1996), The restless, resurgent Campi Flegrei nested caldera (Italy): Constraints on its evolution and configuration, *J. Volcanol. Geotherm. Res.*, *74*, 179–214.

Orsi, G., M. Di Vito, J. Selva, and W. Marzocchi (2009), Long-term forecast of eruption style and size at Campi Flegrei caldera (Italy), *Earth Planet. Sci. Lett.*, *287*, 265–276, doi:10.1016/j.epsl.2009.08.013.

Orsi, G., M. A. Di Vito, and R. Isaia (2004), Volcanic hazard assessment at the restless Campi Flegrei caldera, *Bull. Volcanol.*, *66*, 514–530, doi:10.1007/s00445-003-0336-4.

Orsi, G., G. Gallo, and A. Zanchi (1991), Simple-shearing block resurgence in caldera depressions. A model from Pantelleria and Ischia, *J. Volcanol. Geotherm. Res.*, *47*, 1–11.

Orsi, G., S. Petrazzuoli, and K. Wohletz (1999b), Mechanical and thermo-fluid behaviour during unrest episode at the Campi Flegrei caldera (Italy), *J. Volcanol. Geotherm. Res.*, *91*(2–4), 453–470.

Paoletti V., M. D'Antonio, and A. Rapolla (2013), The structural setting of the Ischia island within the Neapolitan Volcanic area: inferences from geophysics and geochemistry, *J. Volcanol. Geotherm. Res.*, *249*, 155–173, doi:10.1016/j.jvolgeores.2012.10.002.

Reimer, P. J., et al. (2009), IntCal09 and Marine09 radiocarbon age calibration curves, 0–50,000 years Cal BP, *Radiocarbon*, *51*(4), 1111–1150.

Rosi, M., A. Sbrana, and C. Principe (1983), The Phlegrean fields: Structural evolution, volcanic history and eruptive mechanisms, *J. Volcanol. Geotherm. Res.*, *17*, 273–288.

Rymer, H. (1994), Microgravity change as a precursor to volcanic activity, *J. Volcanol. Geotherm. Res.*, *61*, 311–328.

Sacchi, M., G. Alessio, I. Aquino, E. Esposito, F. Molisso, R. Nappi, S. Porfido, and C. Violante (2009), Risultati preliminari della campagna oceanografica CAFE_07–Leg 3 nei Golfi di Napoli e Pozzuoli, Mar Tirreno Orientale, *Quad. Geofis.*, *64*, 25 pp.

Saccorotti, G., S. Petrosino, F. Bianco, M. Castellano, D. Galluzzo, M. La Rocca, E. Del Pezzo, L. Zaccarelli, and P. Cusano (2007), Seismicity associated with the 2004–2006 renewed ground uplift at Campi Flegrei Caldera, Italy, *Phys. Earth Planet. Inter.*, *165*, 14–24. doi:10.1016/j.pepi.2007.07.006.

Sanders, C. O., S. C. Ponko, L. D. Nixon, and E. A. Schwartz (1995), Seismological evidence for magmatic and hydrothermal structure in Long Valley caldera from local earthquake attenuation and velocity tomography, *J. Geophys. Res.*, *100*, 8311–8326.

Scandone, R., F. Bellucci, L. Lirer, and G. Rolandi (1991), The structure of the Campanian Plain and the activity of the Neapolitan volcanoes (Italy), *J. Volcanol. Geotherm. Res.*, *48*, 1–31.

Selva, J., G. Orsi, M. Di Vito, W. Marzocchi, and L. Sandri (2012), Probability hazard map for future vent opening at the Campi Flegrei caldera, Italy, *Bull. Volcanol.*, *74*, 497–510, doi:10.1007/s00445-011-0528-2.

Smith, R. L., and R. A. Bailey (1968), Resurgent cauldrons, *Mem. Geol. Soc. Am.*, *116*, 613–662.

Spilliaert, N., P. Allard, N. Métrich, and A. V. Sobolev (2006), Melt inclusion record of the conditions of ascent, degassing, and extrusion of volatile-rich alkali basalt during the powerful 2002 flank eruption of Mount Etna (Italy), *J. Geophys. Res.*, *111*, B04203, doi:10.1029/2005JB003934.

Tonarini, S., M. D'Antonio, M. A. Di Vito, G. Orsi, and A. Carandente (2009), Geochemical and isotopical (B, Sr, Nd) evidence for mixing and mingling processes in the magmatic system feeding the Astroni volcano (4.1–3.8 ka) within the Campi Flegrei caldera (South Italy), *Lithos*, *107*, 135–151, doi:10.1016/j.lithos.2008.09.012.

Trasatti, E., M. Bonafede, C. Ferrari, C. Giunchi, and G. Berrino (2011), On deformation sources in volcanic areas: Modeling the Campi Flegrei (Italy) 1982–84 unrest, *Earth Planet. Sci. Lett.*, *306*, 175–185.

Vanorio, T., J. Virieux, P. Capuano, and G. Russo (2005), Three-dimensional seismic tomography from P wave and S wave microearthquake travel times and rock physics characterization of the Campi Flegrei Caldera, *J. Geophys. Res.*, *110*, B03201, doi:10.1029/2004JB003102.

Vanorio, T., J. Virieux, A. Zollo, P. Capuano, and G. Russo (2006), A rock physics and seismic tomography study to characterize the structure of the Campi Flegrei Caldera, in *Geophysical Exploration of the Campi Flegrei (southern Italy) Caldera Interiors: Data, Methods and Results*, edited by A. Zollo et al., pp. 25–33, Doppia Voce Editore, Napoli, Italy.

Vassallo, M., A. Zollo, G. Festa, and N. Maercklin (2010), Campi Flegrei (Southern Italy) calderic model from the joint inversion of reflected (PP, PS) and first arrivals seismic traveltimes, E.G.U. General Assembly 2010, *Geophys. Res. Abstr.*, *12*, EGU2010–13157.

Vilardo, G., R. Isaia, G. Ventura, P. De Martino, and C. Terranova (2010), InSAR Permanent Scatterer analysis reveals fault re-activation during inflation and deflation episodes at Campi Flegrei caldera, *Remote Sens. Environ.*, *114*(10), 2373–2383, doi:10.1016/j.rse.2010.05.014.

Yokoyama, I. (1989), Microgravity and height changes caused by volcanic activity: Four Japanese examples, *Bull. Volcanol.*, *51*, 333–345.

Yokoyama, S., and M. Mena (1991), Structure of La Primavera caldera, Jalisco, Mexico, *J. Volcanol. Geotherm. Res.*, *47*, 183–194.

Zhdanov, M. S. (2002), *Geophysical Inverse Theory and Regularization Problems*, Elsevier, 605 pp., Amsterdam, N. Z.

Zollo, A., N. Maercklin, M. Vassallo, D. Dello Iacono, J. Virieux, and P. Gasparini (2008), Seismic reflections reveal a massive melt layer feeding Campi Flegrei caldera, *Geophys. Res. Lett.*, *35*, L12306, doi:10.1029/2008GL034242.